Identifying Factors Influencing Corrosion Rate in Reinforced Concrete under Simulated Natural Climate

Aditi Chauhan[1]* and Umesh Kumar Sharma[2]

1-Department of Civil Engineering, Indian Institute of Technology Bombay, India

2- Department of Civil Engineering, Indian Institute of Technology Roorkee, India

** Corresponding author,*

E-mail address: chauhan.aditi1@gmail.com

Identifying Factors Influencing Corrosion Rate in Reinforced Concrete under Simulated Natural Climate

Abstract

Influence of various parameters on corrosion rate in reinforced concrete was investigated, using Analysis of variance (ANOVA), for crack initiation and crack propagation phases. Water-cement ratio was found to be the most significant factor before the onset of concrete surface crack, followed by the factor: time of wetting. In the crack propagation phase contribution of w/c ratio reduced and factors i.e., time of wetting and external chloride concentration became prominent. Corrosion rate was found to be affected only marginally by the considered concrete cover values of 30 mm and 60 mm. Diameter of reinforcing steel and spacing between bars were the least contributing factors to corrosion rate under both the phases.

***Keywords**: Chloride induced corrosion, corrosion rate, influencing parameters, natural climatic conditions.*

Introduction

Time to corrosion initiation i.e., time for chloride ions to exceed the threshold limit on the rebar and break the passivating layer, has been adopted as service life prediction criteria across the globe [1–4] for quite some time. However, the eventual shift in defining the service life by incorporating the propagation phase led to development of many concrete damage models [5–15] with predefined limit states of cover cracking, loss in steel cross-section, loss in stiffness, loss in structural carrying capacity etc. All these damage models are dependent on a factor defined as corrosion rate (i_{corr}). It is clear from the literature that corrosion rate is a function of various parameters [16–24], and several studies [25–30] have presented ways of quantifying i_{corr} of reinforcing steel in terms of these variables. Many laboratory investigations have been carried out under controlled temperature and relative humidity conditions to quantify the effect of these factors on corrosion propagation, and very few account for the values of corrosion rate in the real environment. Therefore, it becomes necessary to determine the effect of various parameters on i_{corr} under natural environment and develop a model representative of actual i_{corr} in reinforced concrete (RC) structures. To address this, present study will help in identifying the most influential parameters affecting corrosion rate in RC, under laboratory simulated natural climatic variations. Taguchi method of design and analysis was used in the study to identify the factors contributing to corrosion propagation period that was further divided into two phases: crack initiation and crack propagation.

Experimental Procedure

This section details the materials used, fabrication of test specimens and accelerated corrosion test procedure adopted to achieve the desired aim.

Materials

Ordinary Portland cement (OPC) available in the Indian market was used to prepare all the concrete mixtures. This was combined with potable water, river sand, and graded crushed granite with maximum grain sizes of 20 mm and 12.5 mm in the ratio of 1.5 to 1.

Accelerated Corrosion test

Prepared RC specimen with three TMT steel bars i.e., two corner and one middle bar is shown in **Error! Reference source not found.**. To achieve the target crack width of 0.3 mm in the RC specimens under chloride induced corrosion, accelerated corrosion test procedure was adopted. Stainless steel rod of 10 mm diameter which acted as the cathode in accelerated corrosion tests was placed below the middle steel bar at a constant spacing in all the specimens (**Error! Reference source not found.**). Alternate wet-dry cycles with impressed voltage were used to accelerate the corrosion process in the test specimens.

To account for the effect of natural climate on corrosion process, the testing was carried out in a laboratory environment chamber simulating daily variations in temperature and relative humidity (T-RH) for a typical Indian marine city. Similar climatic conditions are found in marine cities located in the north of Australia, west of Brazil, south west of Mexico and in some centrally located African countries. Wet-dry cycles to simulate corrosion in the RC specimens were achieved by wetting the specimens with salt solution and then allowing them to dry in the chamber climatic conditions (Fig. 2). Simultaneous application of impressed constant voltage of 15 volts during wetting cycles was achieved using external Direct Current (DC) supply. Once wetting period for a specimen was completed in a weekly cycle, drying period was maintained for the remaining duration. Fig. 2 shows the schematic of the experimental setup adopted in this study.*

Corrosion rate for each specimen were determined, details of which are provided in the following section.

Design of experiments (Taguchi design)

The present experimental study uses orthogonal array as given by Taguchi to analyze the experimental design and to determine the order in which various parameters influence corrosion rate.

Design parameters and levels

It is imperative to consider the effect of environmental factors along with the material and geometric properties of the structural elements, while carrying out service life studies of RC structures. Table 1 lists the parameters chosen at two different levels to carry out the analysis. The present case limits the number of levels for each parameter to two and can be increased to three or four levels depending on the availability of time and space.

Taguchi design using the defined parameters and levels was prepared as shown in Table 2. Eight set of experiments denoted by E-X, where X refers to the experiment number i.e., from 1 to 8 were analyzed for corrosion rate. Three identical specimens were tested for accelerated corrosion under each experiment.

Experimentation

Accelerated corrosion testing was conducted on the RC specimens in the environmental chamber simulating temperature and relative humidity variations as already explained in the previous section. To shorten the corrosion initiation phase, the specimens were initially subject to electro-migration of chloride ions under 30 Volt as given by [31].

Reference electrode silver/silver chloride electrode was used for measurement of Half Cell Potential (HCP) values on each specimen. It was noted that the HCP values reached the threshold for corrosion activity i.e., -250 mV [32] for all specimens almost after a week. This was followed by accelerated corrosion tests under impressed voltage of 15 volts and wet-dry cycles, to determine corrosion rate, that was determined for all three steel bars in each specimen using galvanostatic pulse method (GPM) based device, at the end of every wet-dry cycle. In addition to the corrosion rate, concrete surface crack width values were also measured weekly using crack measuring microscope with a least count of 0.05 mm.

Results and Discussion

Analysis of Taguchi Design

Analysis of present Taguchi experimental design was carried out for corrosion rate values in two different phases. As suggested by [20] corrosion rate values were averaged up to the point when crack width reaches a value of 0.3 mm. Average values of corrosion rate were determined separately for corner bars and middle bar under each phase and analysis of the experimental design was performed for these bars.

Table 2 shows the results of corrosion rate for the developed set of experiments under both the phases. Using the average test values presented in Table 2, it is possible to determine the effect of individual parameters at different levels on corrosion rate. The mean of corrosion rate for corner bars at a specified level is calculated and termed the level mean average. Here, level mean average for parameter A at level 1 was found to be 0.88 under Phase-1 using the average values of the means (0.69, 0.57, 1.46 and 0.80) taken from E-1, E-2, E-3 and E-4. Similarly, the level mean averages of each design parameter at different levels indicating representative values of corrosion rate in corner and middle bars for Phase-1 and Phase-2 are given in Table 3.

The difference between the maximum and minimum level mean average gave ranks, which indicated the order of the influence of the six design parameters on corrosion rate in both phases, are also given in Table 3. It is clear from the table that the ranking of the parameters gets changed when corrosion propagates from Phase-1 to Phase-2.

Analysis of Variance (ANOVA)

Once the ranks of the all the parameters were determined for both the phases, it was important to evaluate the contribution of each parameter on corrosion rate quantitatively. This was accomplished by ANOVA analysis to predict percentage contribution of each parameter on corrosion rate which was determined using equation 1 and is provided in Table 4 for corner and middle bars under both the phases.

$$\text{Percentage contribution of each parameter} = \frac{SSK}{SST} \times 100 \qquad (2)$$

ANOVA analysis indicates that the percentage contribution of different parameters varied with the occurrence of cracks in the RC specimens.

Effect of time of wetting

It was observed that increasing the time of wetting increased the corrosion rate value as shown in Fig. 3. An increase in the time of wetting exposed the specimen to the corroding environment for a longer duration. A previous research [33] found an inverse relationship between the time of wetting and corrosion rate. This is due to more availability of oxygen during larger drying periods for cathodic reactions to take place, and therefore results in higher value of corrosion rate. In this study, the specimens were subjected to variations in climate during drying period representative of a typical marine city of subcontinent, which is characterized by high relative humidity. Concrete pores got blocked at high relative humidity resulting in discontinuity of interconnected pores and therefore shortage of oxygen in such environment.

Effect of external chloride concentration

In the present study corrosion rate for un-cracked concrete i.e., during Phase-1 remained unaffected by varying the external chloride concentration values between 3.5% and 5% (Table 4). However, during Phase-2, dependence of chloride concentration on corrosion rate increased as observed from Table 4. For cracking phase, the reinforcing steel bars came in direct contact with the external environment i.e., salt solution, through cracks running from concrete surface to the rebar surface. Electrochemical cell potential being dependent on the concentration of the electrolyte allowed change in anodic and cathodic potential on the rebar surface and therefore affected corrosion rate values. An increase in the salt concentration resulted in higher corrosion rate values for both the side and middle bars after cracking.

Effect of w/c ratio

Lower corrosion rate was observed at w/c ratio of 0.4 as compared to at w/c 0.5, which is clearly evident from the slope of the line in Fig. 3. The contribution of w/c ratio was found to be highest amongst all the factors considered in the study, during Phase-1, as shown in Table 4. During Phase-2, influence of w/c ratio reduced considerably, as shown in Table 4.

Effect of concrete cover depth

In the present study, for the adopted cover depth values of 30 mm and 60 mm, reduction in i_{corr} was lesser with the increase in cover thickness. Concrete cover affects the corrosion rate mainly by governing the travel path of the corrosion agents (oxygen, moisture), but the present case suggests that this parameter has a lower effect in comparison to w/c ratio. Similar observations were made by [19] for concrete cover thicknesses of 50 mm and 100 mm along with w/c ratio of 0.4 and 0.7. The values chosen for cover depth in the present study and by [19] are higher than the minimum required cover given in the design codes. Therefore, it would be appropriate to conclude here that corrosion rate values are not affected much by concrete cover values of greater than 30 mm.

Effect of rebar diameter

The present investigation shows a reduction in corrosion rate values for a 12 mm reinforcing bar in comparison to 8 mm bar (**Error! Reference source not found.**). ANOVA analysis shows a very small contribution of rebar diameter to corrosion rate for both side and middle bars before and after cracking.

Effect of spacing between bars

The analysis showed that an increase in the spacing slightly increased the corrosion rate value (Fig. 3). However, variations in the response using chosen spacing values were found to be insignificant compared as compared to other variables of the study (Table 4).

Conclusions

Taguchi design of experiments was implemented to investigate the effect of various key parameters on corrosion rate in reinforced concrete under laboratory simulated natural climatic conditions. Rate of corrosion in two phases of corrosion propagation i.e., before the onset of surface crack and when the crack width reaches a value of 0.3 mm, were analyzed using Taguchi analysis and ANOVA. Following conclusions can be drawn from the results.

1. Water cement (w/c) ratio is the most significant factor influencing corrosion rate before the onset of surface crack and its contribution decreases with the appearance of concrete surface cracks.
2. Time of wetting of RC structures also influences corrosion rate before the initiation of cracking in the form that larger the wetting time higher is the corrosion rate. Even after the onset of cracking, this environmental parameter has a significant effect on corrosion rate and therefore should be considered in the durability design.
3. External chloride concentration, diameter of reinforcing bar and spacing between have been found to have a negligible effect on corrosion rate before surface cracking. However, with the onset of surface cracking their influence on corrosion rate increases and chloride concentration is the most contributing amongst other factors.
4. Corrosion rate is not affected much by the range of concrete cover values (30 mm and 60 mm) or the spacing between the bars (43 mm and 68 mm) chosen in this study.

5. High relative humidity in the environment results in higher rate of corrosion for shorter drying period. This trend is opposite to what has been observed in most of the previous investigations suggesting the importance of considering the natural climatic conditions while performing corrosion rate estimation.

References

1. de Medeiros-Junior, R. A., de Lima, M. G., and de Medeiros, M. H. F., Service life of concrete structures considering the effects of temperature and relative humidity on chloride transport. *Environ. Dev. Sustain.*, 2014, **17**, 1103–1119.

2. Liang, M. T., Wang, K. L., and Liang, C. H., Service life prediction of reinforced concrete structures. *Cem. Concr. Res.*, 1999, **29**, 1411–1418.

3. Bentz, E. C., Probabilistic modeling of service life for structures subjected to chlorides.pdf. *ACI Mater. J.*, 2003, **100**, 391–397.

4. Jiao, J. T., Ye, Y. H., Wang, C. F., and Ye, G. C., The Reliability Analysis of the Initiation Time for RC Members under Chlorine Salt Ingress and Local Micro-Climate. *Mater. Sci. Forum*, 2016, **866**, 134–138.

5. Nossoni, G., Asce, A. M., Harichandran, R. S., and Asce, F., Electrochemical-Mechanistic Model for Concrete Cover Cracking Due to Corrosion Initiated by Chloride Diffusion. *J. Mater. Civ. Eng.*, 2014, **26**.

6. Cao, C., Cheung, M. M. S., and Chan, B. Y. B., Modelling of interaction between corrosion-induced concrete cover crack and steel corrosion rate. *Corros. Sci.*, 2013, **69**, 97–109.

7. Chen, E. and Leung, C. K. Y., A coupled diffusion-mechanical model with boundary element method to predict concrete cover cracking due to steel corrosion. *Corros. Sci.*, 2017, **126**, 180–196.

8. Zhao, Y., Dong, J., Wu, Y., and Jin, W., Corrosion-induced concrete cracking model considering corrosion product-filled paste at the concrete/steel interface. *Constr. Build. Mater.*, 2016, **116**, 273–280.

9. Ožbolt, J., Oršani, F., and Balabani, G., Modeling damage in concrete caused by corrosion of reinforcement : coupled 3D FE model. *Int. J. Fract.*, 2012, **178**, 233–244.

10. Michel, A., Geiker, M. R., Stang, H., and Lepech, M. D., Integrated modelling of corrosion-induced deterioration in reinforced concrete structures. *EuroCorr*, 2013, 1–5.

11. Thybo, A. E. A., Michel, A., and Stang, H., Smeared crack modelling approach for corrosion-induced concrete damage. *Mater. Struct.*, 2017, **50**, 1–14.

12. Dagher, H. and Kulendran, S., Finite element modeling of corrosion damage in concrete structures. *ACI Struct. J.*, 1992, **89**, 699–708.

13. Guzman, S., Galvez, J. C., and Sancho, J. M., Modelling of corrosion-induced cover cracking in reinforced concrete by an embedded cohesive crack finite element. *Eng. Fract. Mech.*, 2012, **93**, 92–107.

14. Zhang, J., Ling, X., and Guan, Z., Finite element modeling of concrete cover crack propagation due to non-uniform corrosion of reinforcement. *Constr. Build. Mater.*, 2017, **132**, 487–499.

15. Jamali, A., Angst, U., Adey, B., and Elsener, B., Modeling of corrosion-induced concrete cover cracking: A critical analysis. *Constr. Build. Mater.*, 2013, **42**, 225–237.

16. Otieno, M., Beushausen, H., and Alexander, M., Prediction of Corrosion Rate in RC Structures - A Critical Review. In *Modelling of Corroding Concrete Structures* 2011.

17. Scott, A. and Alexander, M. G., The influence of binder type , cracking and cover on corrosion rates of steel in chloride- contaminated concrete. *Mag. Concr. Res.*, 2007, **59**, 495–505.

18. Balabanić, G., Bićanić, N., and Dureković, A., MATHEMATICAL MODELING OF ELECTROCHEMICAL STEEL CORROSION IN CONCRETE. *J. Eng. Mech.*, 1996, **122**, 1113–1122.

19. Balabanić, G., Bićanić, N., and Dureković, A., The influence of w/c ratio, concrete cover thickness and degree of water saturation on the corrosion rate of reinforcing steel in concrete. *Cem. Concr. Res.*, 1996, **26**, 761–769.

20. Otieno, M. B., Alexander, M. G., and Beushausen, H.-D., Corrosion in cracked and uncracked concrete – influence of crack width, concrete quality and crack reopening. *Mag. Concr. Res.*, 2010, **62**, 393–404.

21. Isgor, O. B. and Ghods, P., The effect of temperature on the corrosion of steel in concrete . Part 1 : Simulated polarization resistance tests and model development. *Corros. Sci.*, 2009, **51**, 415–425.

22. Hervert, H. L. Z. and Mendez, R. C., Identifying Factors Influencing the Corrosion Rate of Steel Using Nonparametric Statistics. *Int. J. Electrochem. Sci.*, 2012, **7**, 6343–6352.

23. Villagrán Zaccardi, Y. a., Bértora, a., and Di Maio, Á. a., Temperature and humidity influences on the on-site active marine corrosion of reinforced concrete elements. *Mater. Struct.*, 2013, **46**, 1527–1535.

24. Otieno, M., Beushausen, H., and Alexander, M., Chloride-induced corrosion of steel in cracked concrete – Part I : Experimental studies under accelerated and natural marine environments. *Cem. Concr. Res.*, 2016, **79**, 373–385.

25. Liu, Y. and Weyers, R. E., Modeling the time-to-corrosion cracking in chloride contaminated reinforced concrete structures. *ACI Mater. J.*, 1998, **95**, 675–681.

26. Raupach, M., Models for the propagation phase of reinforcement corrosion – an overview. *Mater. Corros.*, 2006, **57**, 605–613.

27. Mart, B., Service life modelling of reinforced concrete structures exposed to chlorides. *PhD Thesis*, 1999.

28. Jung, W. Y., Yoon, Y. S., and Sohn, Y. M., Predicting the remaining service life of land concrete by steel corrosion. *Cem. Concr. Res.*, 2003, **33**, 663–677.

29. Vu, K. A. T. and Stewart, M. G., Structural reliability of concrete bridges including improved chloride-induced corrosion models. *Struct. Saf.*, 2000, **22**, 313–333.

30. Otieno, M., Beushausen, H., and Alexander, M., Chloride-induced corrosion of steel in cracked concrete - Part II: Corrosion rate prediction models. *Cem. Concr. Res.*, 2016, **79**, 386–394.

31. Xia, J., Jin, W.-L., and Li, L.-Y., Effect of chloride-induced reinforcing steel corrosion on the flexural strength of reinforced concrete beams. *Mag. Concr. Res.*, 2012, **64**, 471–485.

32. John H. Bungey, S. G. M. and M. G. G., *Testing of Concrete in Structures* taylor and Francis, 2006.

33. Gavin Golden, The effect of cyclic wetting and drying on the corrosion rate of steel in

reinforced concrete . *MS Thesis*, 2015.

Table 1. Factors and levels for Taguchi design and analysis

Factors	Level 1	Level 2
A: Time of wetting (TOW) (days)	3	5
B: Chloride concentration (CONC.) (%)	3.5	5
C: Water cement ratio (w/c)	0.4	0.5
D: Concrete cover depth (cover) (mm)	30	60
E: Diameter of rebar (dia) (mm)	8	12
F: Spacing between rebars (spacing) (mm)	48	63

Table 2. Taguchi design with results for corrosion rate

	FACTORS						Phase-1		Phase-2	
Experiment	A	B	C	D	E	F	i_{corr} (average of corner bars) ($\mu A/cm^2$)	i_{corr} (middle bar) ($\mu A/cm^2$)	i_{corr} (average of corner bars) ($\mu A/cm^2$)	i_{corr} (middle bar) ($\mu A/cm^2$)
E-1	3	5	0.4	30	8	43	0.69	0.99	0.75	0.91
E-2	3	5	0.4	60	12	68	0.57	0.59	0.59	0.58
E-3	3	3.5	0.5	30	8	68	1.46	1.57	0.68	0.94
E-4	3	3.5	0.5	60	12	43	0.80	1.00	0.56	0.51
E-5	5	5	0.5	30	12	43	1.50	2.13	0.85	1.52
E-6	5	5	0.5	60	8	68	1.61	1.47	1.85	2.07
E-7	5	3.5	0.4	30	12	68	0.96	0.80	0.69	0.56
E-8	5	3.5	0.4	60	8	43	0.96	0.97	0.64	0.67

Table 3. Taguchi analysis results for corner and middle bar showing ranking of parameters

(a) Phase-1 (Corner bar)

Level	TOW	CONC	W/C	COVER	DIA	SPACING
1	0.880	1.045	0.798	1.154	1.180	0.988
2	1.258	1.094	1.341	0.984	0.959	1.151
Delta	0.377	0.049	0.544	0.17	0.222	0.163
Rank	2	6	1	4	3	5

(b) Phase-2 (Corner bar)

Level	TOW	CONC	W/C	COVER	DIA	SPACING
1	0.644	0.641	0.666	0.741	0.977	0.698
2	1.007	1.010	0.985	0.910	0.674	0.953
Delta	0.363	0.370	0.318	0.169	0.304	0.256
Rank	2	1	3	6	4	5

(c) Phase-1 (Middle bar)

Level	TOW	CONC	W/C	COVER	DIA	SPACING
1	1.035	1.082	0.835	1.371	1.248	1.271
2	1.342	1.295	1.542	1.006	1.129	1.106
Delta	0.307	0.212	0.707	0.364	0.118	0.165
Rank	3	4	1	2	6	5

(d) Phase-2 (Middle bar)

Level	TOW	CONC	W/C	COVER	DIA	SPACING
1	0.736	0.672	0.679	0.982	1.146	0.902
2	1.204	1.269	1.261	0.958	0.794	1.038
Delta	0.468	0.597	0.582	0.025	0.352	0.136
Rank	3	1	2	6	4	5

Table 4. ANOVA analysis results for corner and middle bars

(a) Phase-1 (Corner bar)

Source	Sum of Squares (SSK)	Mean Square	F-Value	%age contribution
A: Time of wetting (days)	0.285	0.285	12.75	25.60
B: Chloride concentration (%)	0.005	0.005	0.22	0.44
C: Water cement ratio	0.591	0.591	26.47	53.15
D: Concrete cover depth (mm)	0.058	0.058	2.59	5.20
E: Diameter of rebar (mm)	0.098	0.098	4.4	8.83
F: Spacing between rebars (mm)	0.053	0.053	2.38	4.79
Error	0.022	0.022	-	-
Total (SST)	1.113	-	-	-

(b) Phase-2 (Corner bar)

Source	Sum of Squares (SSK)	Mean Square	F-Value	% age contribution
A: Time of wetting (days)	0.264	0.264	1.77	20.92
B: Chloride concentration (%)	0.273	0.273	1.83	21.66
C: Water cement ratio	0.203	0.203	1.36	16.05
D: Concrete cover depth (mm)	0.057	0.057	0.38	4.55
E: Diameter of rebar (mm)	0.185	0.185	1.24	14.64
F: Spacing between rebars (mm)	0.131	0.131	0.87	10.34
Error	0.149	0.149	-	-
Total (SST)	1.262	-	-	-

(c) Phase-1 (Middle bar)

Source	Sum of Squares (SSK)	Mean Square	F-Value	%age contribution
A: Time of wetting (days)	0.189	0.189	1.49	10.77
B: Chloride concentration (%)	0.090	0.090	0.71	5.13
C: Water cement ratio	1.000	1.000	7.88	57.02

D: Concrete cover depth (mm)	0.265	0.265	2.09	15.13
E: Diameter of rebar (mm)	0.028	0.028	0.22	1.59
F: Spacing between rebars (mm)	0.055	0.055	0.43	3.12
Error	0.127	0.127		-
Total	1.754			-

(d) Phase-2 (Middle bar)

Source	Sum of Squares (SSK)	Mean Square	F-Value	%age contribution
A: Time of wetting (days)	0.438	0.438	32.08	20.57
B: Chloride concentration (%)	0.713	0.713	52.25	33.50
C: Water cement ratio	0.678	0.678	49.69	31.86
D: Concrete cover depth (mm)	0.001	0.001	0.09	0.06
E: Diameter of rebar (mm)	0.248	0.248	18.15	11.64
F: Spacing between rebars (mm)	0.037	0.037	2.70	1.73
Error	0.014	0.014	-	-
Total	2.129	-	-	-

List of Figures

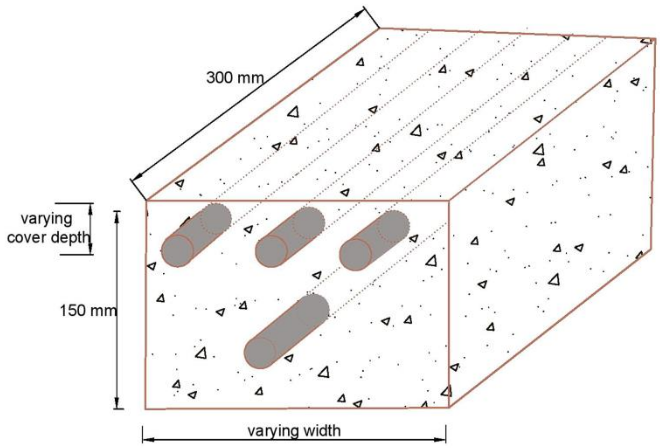

Fig. 1 Reinforced concrete specimen subject to corrosion

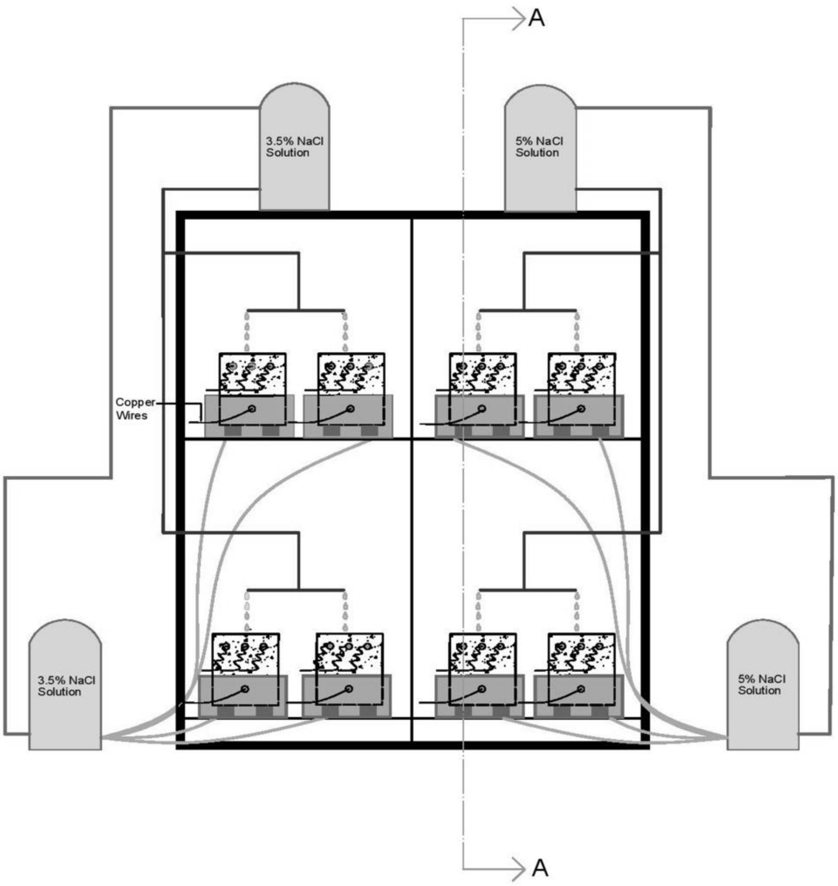

(a) Section showing corrosion setup inside the environment chamber

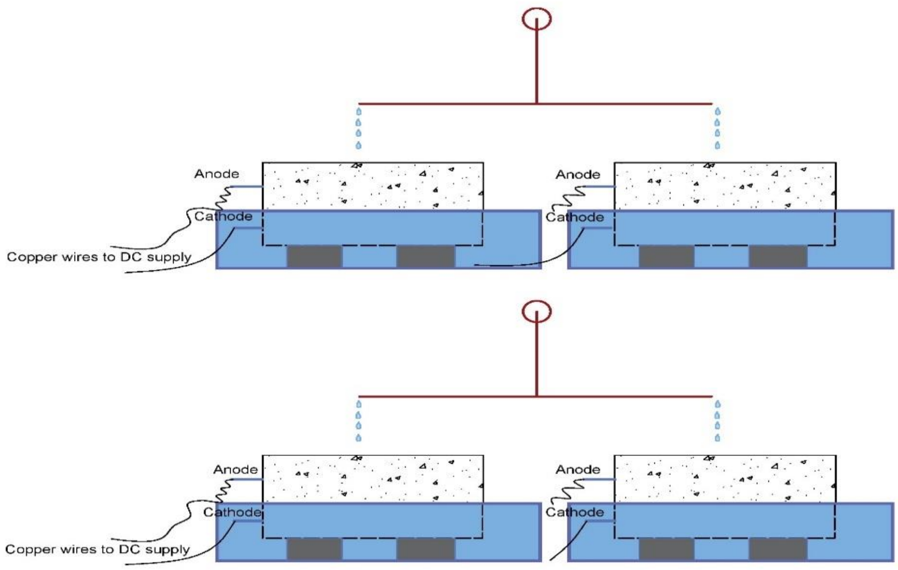

(b) Section A-A

Fig. 2 Schematic of experimental setup to carry out Taguchi Design of Experiments

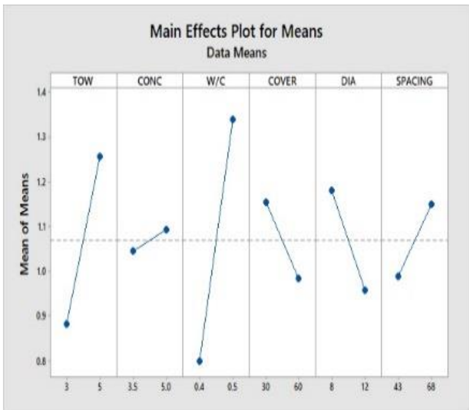

(a) corner bars_Phase-1

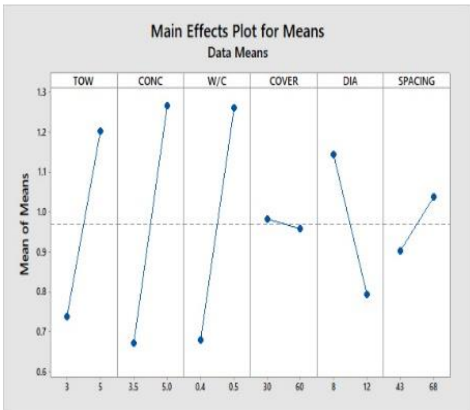

(b) corner bars_Phase-2

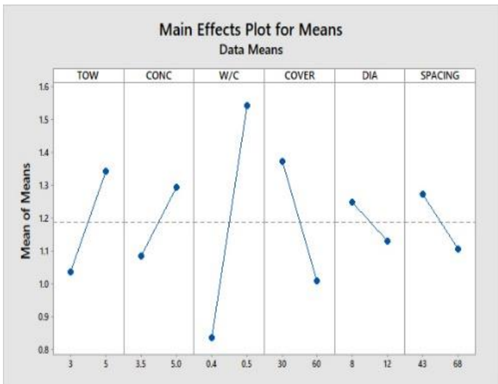

(c) middle bar_Phase-1

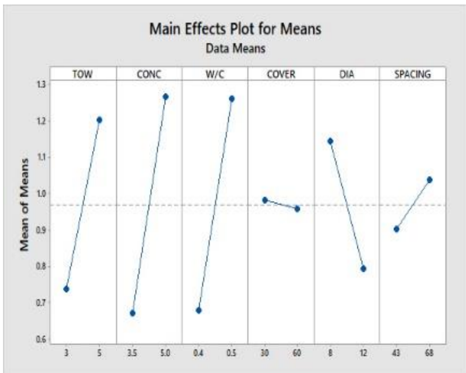

(d) middle bar_ Phase-2

Fig. 3 Effect of various parameters on corrosion rate before and after appearance of surface cracks